JTTEE5 16:791–797
DOI: 10.1007/s11666-007-9093-9
1059-9630/$19.00 © ASM International

Yttria-Stabilized Zirconia Thermal Barriers Sprayed Using N_2-H_2 and Ar-H_2 Plasmas: Influence of Processing and Heat Treatment on Coating Properties

B.R. Marple, R.S. Lima, C. Moreau, S.E. Kruger, L. Xie, and M.R. Dorfman

(Submitted March 9, 2007)

Thermal barrier coatings were produced using both Ar and N_2 as the primary plasma gas. Various aspects of the process and the coatings were investigated. It was found that higher in-flight particle temperatures could be produced using N_2, but particle velocities were lower. Deposition efficiencies could be increased by a factor of two by using N_2 as compared to Ar. Coatings having similar values of porosity, hardness, Young's modulus, and thermal diffusivity could be produced using the two primary gases. The coatings exhibited similar changes (increased hardness, stiffness, and thermal diffusivity) when heat-treated at 1400 °C. However, the N_2-processed coatings tended to have lower values of Young's modulus and thermal diffusivity following such treatment. The results point to the potential advantage, in terms of reduced powder consumption and increased production rate, of using N_2 as compared to Ar as the primary plasma gas for TBC deposition.

Keywords deposition efficiency, elastic properties, in-flight particle characteristics, nitrogen-hydrogen plasmas, thermal barrier coating, thermal diffusivity, thermal treatment

1. Introduction

Thermal barrier coatings (TBCs) are widely used on gas turbine components employed in both aerospace and industrial gas turbine applications (Ref 1). The most commonly employed composition for producing the insulating ceramic top coat of these structures is a zirconia-based material, containing 7-8 wt.% yttria (Y_2O_3) to stabilize the phase structure. The coatings can be applied by different routes, including air plasma spraying (APS), where a wide range of spray systems and deposition conditions can be employed.

As with most products, cost and quality are key issues at all points along the manufacturing process for these coatings. The goal is to minimize cost while producing coatings that meet the requirements of the application. Quality also includes the ability to consistently deposit coatings in a reproducible manner to meet the design specifications.

The present study involved aspects relating to both quality and cost. For producing TBCs by APS, two main plasma gas mixtures are currently being employed: argon/hydrogen (Ar/H_2), which has been the traditional approach, and nitrogen/hydrogen (N_2/H_2). Once an APS processing route has been established, many producers are reluctant to make major changes to this accepted approach. The reasons for this are based on the potentially high cost should the coatings produced using the new approach fail in service.

Published work has shown the potential for obtaining relatively high deposition efficiency (DE) using N_2/H_2 as the plasma gas (Ref 2). Deposition efficiency is an important parameter when calculating the coating cost: increasing DE reduces powder consumption and can increase the rate of production. In this paper, details of a study that investigated aspects relating to the APS processing of TBCs using N_2/H_2 as the plasma gas, characterization of the microstructure of the resulting coatings, and evaluation of various properties of the as-sprayed and heat-treated coatings are reported. These results are compared to those obtained for Ar/H_2-processed TBCs.

This article is an invited paper selected from presentations at the 2007 International Thermal Spray Conference and has been expanded from the original presentation. It is simultaneously published in *Global Coating Solutions, Proceedings of the 2007 International Thermal Spray Conference*, Beijing, China, May 14-16, 2007, Basil R. Marple, Margaret M. Hyland, Yuk-Chiu Lau, Chang-Jiu Li, Rogerio S. Lima, and Ghislain Montavon, Ed., ASM International, Materials Park, OH, 2007.

B.R. Marple, R.S. Lima, C. Moreau, and **S.E. Kruger**, Industrial Materials Institute, National Research Council of Canada, Boucherville, QC, Canada; and **L. Xie** and **M.R. Dorfman**, Sulzer Metco (US) Inc., Westbury, NY, USA. Contact e-mail: basil.marple@cnrc-nrc.gc.ca.

2. Experimental Procedure

2.1 APS Processing and Particle Diagnostics

All experiments were performed using a commercially available 8 wt.% yttria-stabilized zirconia (8YSZ) hollow

spherical powder (HOSP) in the size range 45-75 μm (204B-NS, Sulzer Metco Inc., Westbury, NY, USA). Thermal spraying was carried out employing a plasma torch (9MB, Sulzer Metco Inc., Westbury, NY, USA) and a wide range of spray parameter settings. Experiments were performed using both Ar/H_2 and N_2/H_2 as the plasma gas mixture. Because of the thermal properties and viscosities of these gases, Ar/H_2 plasmas tend to produce particle jets that are cooler and faster than those arising with N_2/H_2 plasmas.

Initially, the spray parameters were varied in order to sample a large region of the temperature-velocity (*T-V*) space for the in-flight particles. In the case of Ar/H_2, this involved mainly changes in the current, power, hydrogen flow rate, spray distance, and powder feed rate. For the N_2/H_2 plasma gas, the current, powder feed rate, spray distance, hydrogen flow rate, and carrier gas flow were the main variables for producing changes in the in-flight particle characteristics. These changes were monitored using diagnostic equipment (Accuraspray-g[3], Tecnar Automation Ltd., St. Bruno, Quebec, Canada) to determine the average temperature and velocity of particles at the selected standoff distance in the thermal spray jet. Based on these initial measurements, approximately ten sets of spray parameters were selected for each of the two gas mixtures for coating production and further investigation. The first step involved measuring the DE. This was determined for each set of coating conditions by depositing on substrates of the same composition (mild steel) as used in producing samples. Deposition on these grit-blasted substrates of known dimensions was performed using a pre-determined powder feed rate, torch speed, and total number of passes. The DE could be calculated by comparing the weight of the substrate before and after the deposition with respect to the powder feed rate. Coatings were then produced for determining the hardness, thermal diffusivity, and elastic properties and comparing the microstructures and levels of porosity. From these results, several coatings were chosen for a thermal treatment, followed by a re-evaluation of the various properties mentioned above.

2.2 Thermal Treatment

Thermal treatments were performed on coatings to determine the effect of temperature on the properties and microstructure. These treatments were carried out on free-standing coatings that had been removed from the mild steel substrates by dissolving the metal base. The thickness of the coatings ranged from ~350 μm to ~550 μm, depending on what measurements were to be performed using a given sample. Heating was accomplished in air in a box furnace by commencing at room temperature and increasing to 1400 °C over a 60-90 min period. Samples were left at this temperature for dwell times of 1, 5, and 20 h, following which they were removed from the furnace and allowed to cool. Initial cooling was very rapid and, typically, room temperature was reached within 30 min.

2.3 Analysis and Characterization of the Coatings

2.3.1 Microstructure. Samples of as-sprayed and heat-treated coatings were mounted in epoxy resin using vacuum impregnation and then sectioned. The cross sections were polished using standard metallographic techniques. Samples were studied under a scanning electron microscope (SEM) (Model S4700, Hitachi Instruments Inc., Tokyo, Japan) to observe the microstructure. The level of porosity was determined with the aid of image analysis software (NIH *Image*, public domain software, National Institutes of Health (NIH), USA) on images obtained (at a magnification of 500×) using a scanning electron microscope (JSM-6100, JEOL, Tokyo, Japan) in the backscattered mode under conditions of contrast to enhance the appearance of pores. An average value of porosity was determined for each coating from the results of separate analyses from ten regions within the cross section.

2.3.2 Hardness. Two different hardness values were measured for the coatings. For these tests, coatings were deposited to a thickness >500 μm. The Rockwell superficial hardness value (HR15N) of as-sprayed coatings was determined by indenting the top surface with a diamond cone under a total mass of 15 kg (force = 147.1 N). Results from five such indentations were used to calculate an average HR15N value for each coating. No such measurements could be made on coatings removed from the substrate because the free-standing samples fractured under the indenter.

The Vickers microhardness number ($HV_{0.3}$) was determined using a microhardness tester (Micromet II, Buehler, Lake Bluff, IL, USA). Average values of the microhardness number on the cross section of as-sprayed and heat-treated coatings were calculated using data from ten indentations made under a 300 g load. It should be noted that because the porosity in the coatings was infiltrated with epoxy, the microhardness number is that of the composite epoxy/coating material. Therefore, the values should be used simply for ranking the different coatings and providing a basis for identifying changes in the relative microhardness caused by heat treatment.

2.3.3 Thermal Diffusivity. The thermal diffusivity of the coatings was determined by the laser flash method using an experimental set-up described elsewhere (Ref 3). Measurements were made on coatings having a thickness of ~400 μm that had been removed from the substrate.

2.3.4 Elastic Properties. The elastic properties were investigated using laser ultrasonic measurements on free-standing coatings having a length of 51 mm, a width of 25 mm, and a thickness in the range of 500-600 μm. The technique, which was similar to that employed in earlier work on WC-Co coatings (Ref 4), involved the generation of ultrasonic waves by a Nd:YAG (third harmonic: 355 nm) laser pulse focused in a line (~200 μm × 5 mm) in the coating surface. The waves were detected about 6 mm away in the same surface by a long pulse Nd:YAG (1064 nm) also focused in a line geometry. The scattered detection light was demodulated by a GaAs photorefractive interferometer. By measuring the time arrival of the

fundamental symmetric wave mode (S0), the elastic constant could be calculated. This approach was employed to determine the Young's modulus (E) value for coatings both before and following thermal treatment. It should be noted that the values of Young's modulus reported here should not be taken as absolute; rather, the data allows comparison of the different coatings and provides a basis for determining the relative effect of the various heat treatments on the elastic properties.

3. Results and Discussion

3.1 Particle Diagnostics and APS Process Parameter Selection

Plots showing the relatively large region of *T-V* space sampled by varying the spray parameters are shown in Fig. 1 for both plasma gas mixtures. These plots indicate that conditions resulting in the lowest heating of the particles produced similar temperatures (2400-2500 °C) for both gas mixtures. However, for the hottest spray conditions it was possible to reach temperatures ~300 °C higher by using N_2 as the primary gas (~3100 °C) as compared to Ar (~2800 °C). It is also evident that for a given temperature, significantly higher values of particle velocity could be achieved by using Ar. This difference was ~50 m/s. In fact, the highest velocity of ~120 m/s achieved using N_2 occurred at a temperature of ~3100 °C. When using Ar, particle velocities were all above this value for temperatures >2600 °C.

These results can be explained using the properties of the two primary gases. At the plasma temperature, the thermal conductivity of N_2 is 2-3 times higher than that of Ar (Ref 5). Therefore, employing N_2 results in more effective heat transfer to the 8YSZ particles (and higher particle temperatures) than when Ar is the primary plasma gas. However, the viscosity is higher for Ar (Ref 5) and, in these experiments (as is normally the case when using these gases), the total plasma gas flow was greater than when using N_2. This contributes to the particles attaining a higher velocity with Ar plasmas.

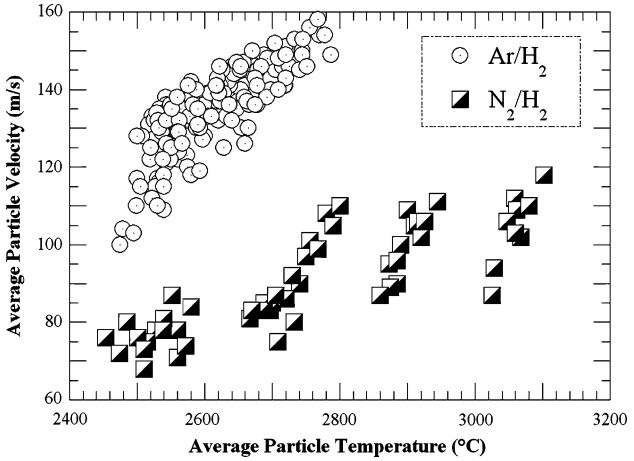

Fig. 1 Region of *T-V* space sampled using a range of APS conditions and Ar and N_2 as primary plasma gases

Using this data, the parameter sets identified in Tables 1 and 2 were chosen for further work. Results of particle diagnostics for these conditions are shown in Fig. 2. The set numbers are indicated in this and subsequent figures to enable comparison and cross-referencing between the various graphs and tables.

3.2 Characterization of As-Sprayed Coatings

Graphs showing the values of DE for the conditions listed in Tables 1 and 2 and of the porosity level and Rockwell superficial hardness of the coatings as a function of the in-flight particle temperature are shown in Fig. 3, 4, and 5. As seen in Fig. 3, the DE tends to increase with the in-flight particle temperature. This is true for both primary plasma gases. The graph shows that for temperatures above ~2800 °C (achievable using N_2 as the primary gas), the DE tends to reach a plateau at values in the range of 60-70%. This plateau occurs because the melting point of the zirconia-based material is ~2700 °C (Ref 6), so when the average particle surface temperature being measured

Table 1 Spraying conditions used with the Ar/H_2 plasma gas

Set	H_2, L/min	*I*, A	*P*, kW	Feed rate, g/min	SD, mm
1A	7.6	500	32.5	30	110
2A	7.6	500	32.5	60	170
3A	9.0	500	35.0	45	140
4A	11.8	500	37.5	30	110
5A	11.8	500	37.5	60	170
6A	9.9	450	31.5	30	110
7A	9.9	450	31.5	45	110
8A	9.9	550	37.7	30	140
9A	9.9	600	41.0	30	110
10A	9.9	600	41.0	60	170

H_2, secondary plasma gas; *I*, current; *P*, input power calculated using voltage measured at the power supply; SD, standoff distance. Fixed parameters: primary gas (Ar) flow rate = 43 L/min, carrier gas (Ar) flow rate = 5.2 L/min (optimum trajectory observed for all conditions)

Table 2 Spraying conditions used with the N_2/H_2 plasma gas

Set	N_2, L/min	H_2, L/min	CGF, N_2, L/min	*I*, A	*P*, kW	Feed rate, g/min	SD, mm
1	34.0	0	5.0	500	32.5	30	110
2	34.0	0	5.0	500	32.5	45	140
3	34.0	0	5.0	500	32.5	60	170
4	34.0	2.4	5.5	500	35.5	30	110
5	34.0	2.4	5.0	500	35.5	45	140
6	34.0	2.4	5.0	500	35.5	60	170
7	34.0	7.1	5.0	450	35.1	30	110
8	34.0	7.1	5.0	450	35.1	45	140
9	34.0	7.1	6.0	450	35.1	60	170
10	34.0	7.1	6.0	600	48.0	30	110
11	35.4	6.6	5.2	460	35.0	92	114
12	35.4	8.0	5.2	500	39.3	46	114

N_2, primary plasma gas; H_2, secondary plasma gas; CGF, carrier gas (N_2) flow; *I*, current; *P*, input power calculated using voltage measured at the power supply; SD, standoff distance

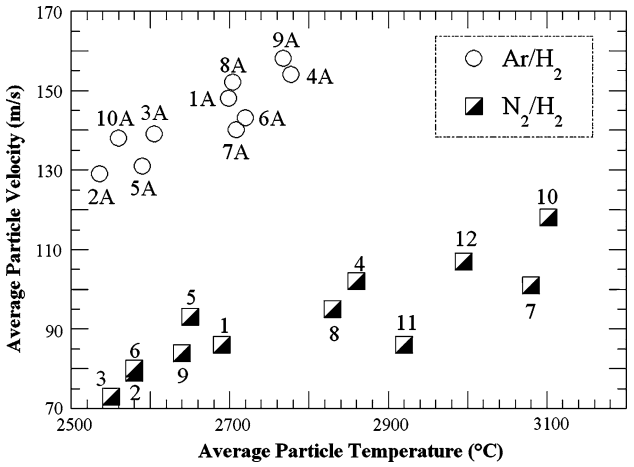

Fig. 2 Conditions for which DE values were measured and, in some cases, for which coatings were produced. The numbers by the data points refer to parameter sets (see Tables 1 and 2)

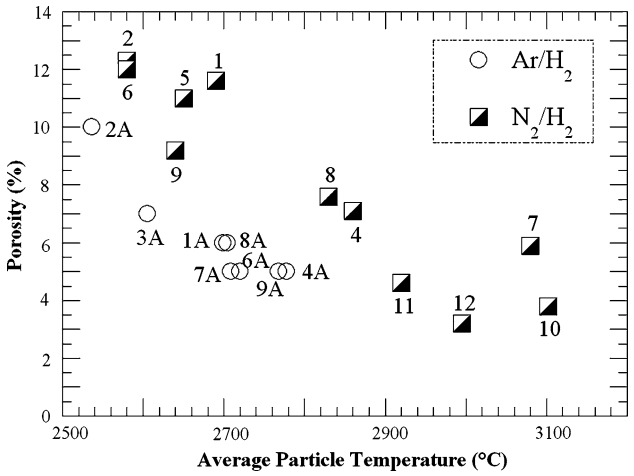

Fig. 4 Porosity level in 8YSZ coatings as a function of in-flight particle temperature for two plasma gases. The standard deviation on the porosity values was ±1-2%

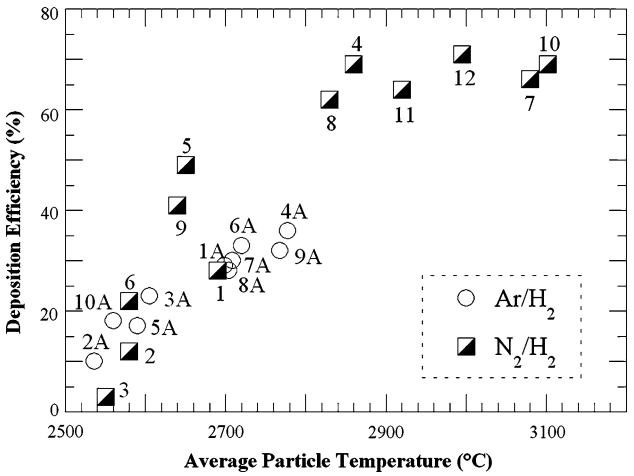

Fig. 3 Deposition efficiency values for APS deposition of 8YSZ using the parameter sets shown in Tables 1 and 2

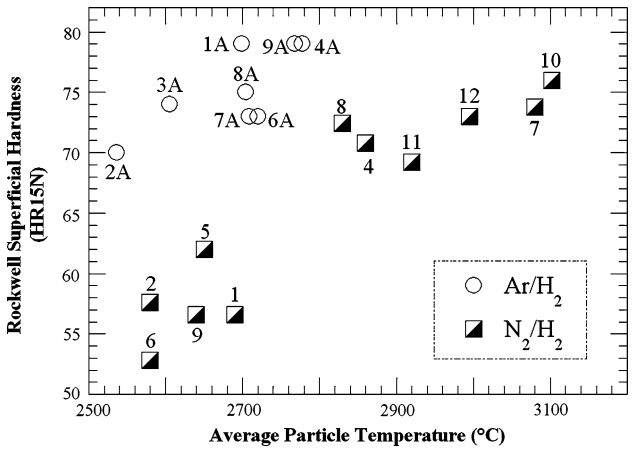

Fig. 5 Hardness values for 8YSZ coatings produced using the parameter sets shown in Tables 1 and 2

by the diagnostic system reaches ~2800 °C it can be assumed that most of the particle cores are molten and additional heating has little effect on the degree of melting. (It should be noted that the diagnostic system provides an average surface temperature value produced by sampling the surface temperatures of a majority of the particle population. Therefore, the cores of these particles (particularly larger particles) are not necessarily molten when the average surface temperature is at the melting point; hence, in some cases, superheating of the particles may be required to bring about complete particle melting.) It is also apparent that much higher DE values can be attained when using N_2 as the plasma gas. The DE can be doubled from 30-35% (Ar) to 60-70% (N_2). This substantial increase has obvious cost (reduction) implications for TBC production.

Figures 4 and 5 show that, as expected, the level of porosity decreases and the hardness increases with increasing in-flight particle temperature. Both of these characteristics are affected by particle velocity, which as shown in Fig. 2, is lower when using N_2 as the primary gas. The graphs indicate that similar porosity and hardness levels can be produced using the two primary gases. In the case of Ar for coatings produced at temperatures above ~2700 °C, the porosity level is 5-6% and the Rockwell superficial hardness is 73-79. For coatings deposited at temperatures above ~2800 °C using N_2, the porosity levels and hardness values are 3.5-7.5% and 69-76%, respectively. However, as noted above, the DE values for producing these coatings was a factor of two higher for N_2.

3.3 Effect of Thermal Treatment

Graphs showing the changes in various properties following the thermal treatment at 1400 °C are presented in Fig. 6, 7, and 8. The changes in the (relative) Vickers

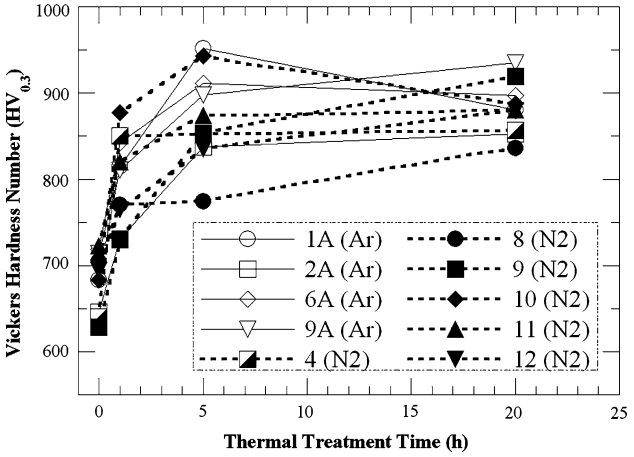

Fig. 6 Vickers hardness numbers of epoxy-infiltrated 8YSZ coatings after various stages of heat treatment at 1400 °C. The legend identifies the parameter sets shown in Tables 1 and 2

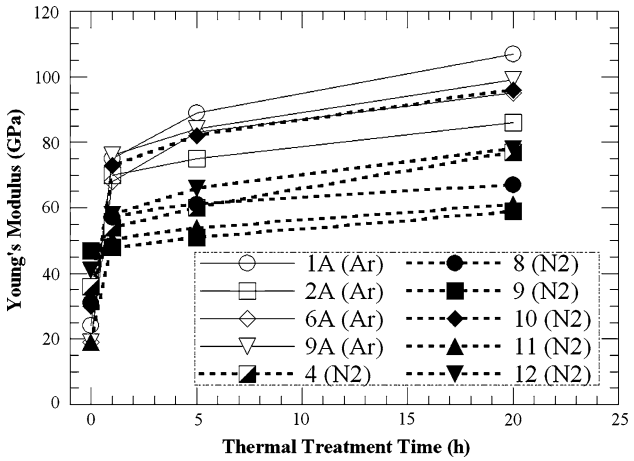

Fig. 7 Effect of thermal treatment at 1400 °C on the Young's modulus of coatings produced using the parameter sets shown in Tables 1 and 2

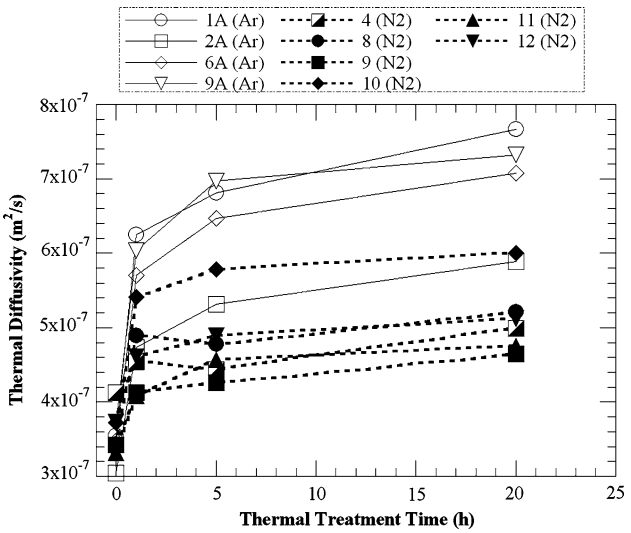

Fig. 8 Effect of thermal treatment at 1400 °C on the thermal diffusivity of coatings produced using the parameter sets shown in Tables 1 and 2

hardness number (Fig. 6) appear to occur in the first 1-5 h of heat treatment for most coatings. The range of initial $HV_{0.3}$ values for the as-sprayed coatings was ~625-725. Following 20 h at 1400 °C, the $HV_{0.3}$ values were in the range ~835-935. No pronounced differences were noted between the coatings produced using N_2 as compared to Ar as primary plasma gas.

The results for Young's modulus (Fig. 7) indicated a similar trend as observed for hardness. The main increases in E occurred during the initial 1-5 h of exposure at 1400 °C; subsequent increases were more gradual. It is worth noting that, in general, the final values of E were lower for coatings produced using N_2 as primary plasma gas as compared to those deposited using Ar. These lower values could indicate more compliant coatings better able to withstand the strains and stresses of high temperature exposure and thermal cycling.

The results for thermal diffusivity (Fig. 8) also show an initial increase after 1-5 h of thermal treatment, followed by a more gradual change. The increases for the coatings produced using N_2 are less than for those deposited using Ar.

The fundamental changes in the coatings during thermal treatment that gave rise to the observed evolution in coating properties were not investigated in detail. Results for porosity levels of the coatings generally indicated little difference between the as-sprayed coatings and those heated for 20 h at 1400 °C. Of course the image analysis technique would not detect the removal of very small pores. It is believed that the observed results of increased hardness, Young's modulus and thermal diffusivity arise due to improved inter-splat bonding and the disappearance of fine inter-splat pores produced by material diffusion at 1400 °C. The smaller increases of Young's modulus and thermal diffusivity after heat treatment for N_2-processed coatings may be related to the higher deposition temperatures used for these coatings. These higher temperatures may have led to a greater extent of reaction of impurities, such that they were less active during the subsequent thermal treatment and played a lesser role in contributing to enhanced inter-splat bonding. A second factor could be differences in localized stress relaxation during thermal treatment. The closure effects (reduced inter-splat distance and increased contact) caused by this relaxation may be less for the N_2-processed coatings where in-flight particle velocities were lower and splat thicknesses likely greater than for the Ar-deposited coatings. Other changes in the coating could also be contributing to produce the observed effects. For example, the phase composition of the coatings has not been investigated in this study. It is known that phase changes can occur in these types of coatings at the thermal treatment temperature employed in this work (Ref 7, 8). Phase changes can be disruptive to the coating structure and affect the properties. It is possible that the differences in the processing conditions resulted in coatings that

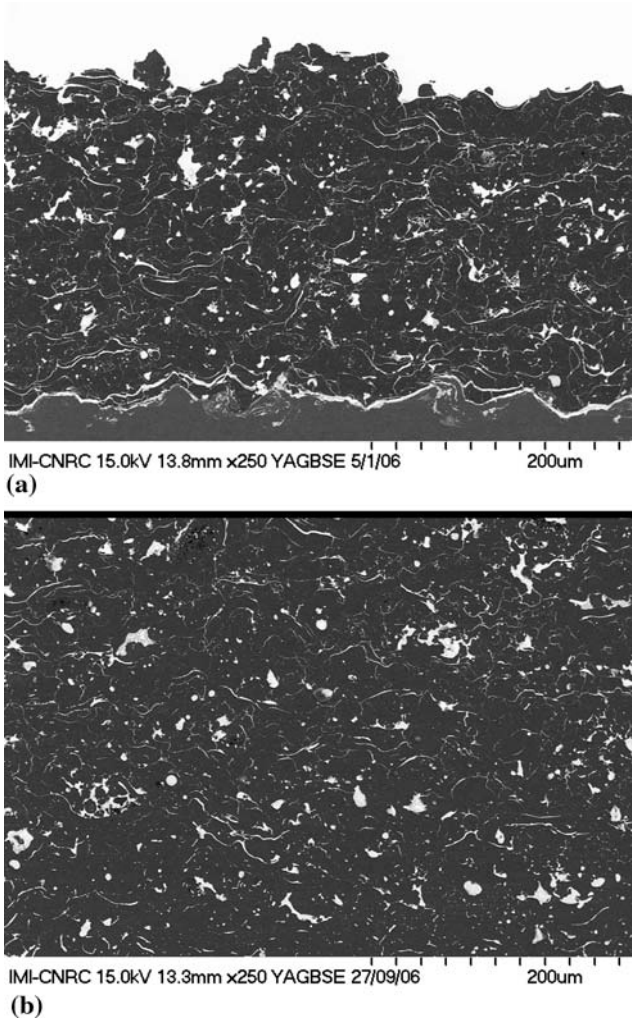

Fig. 9 Microstructure of a coating produced using spray parameter Set 1A (Ar, see Table 1) in the as-sprayed state (a) and following 20 h at 1400 °C (b)

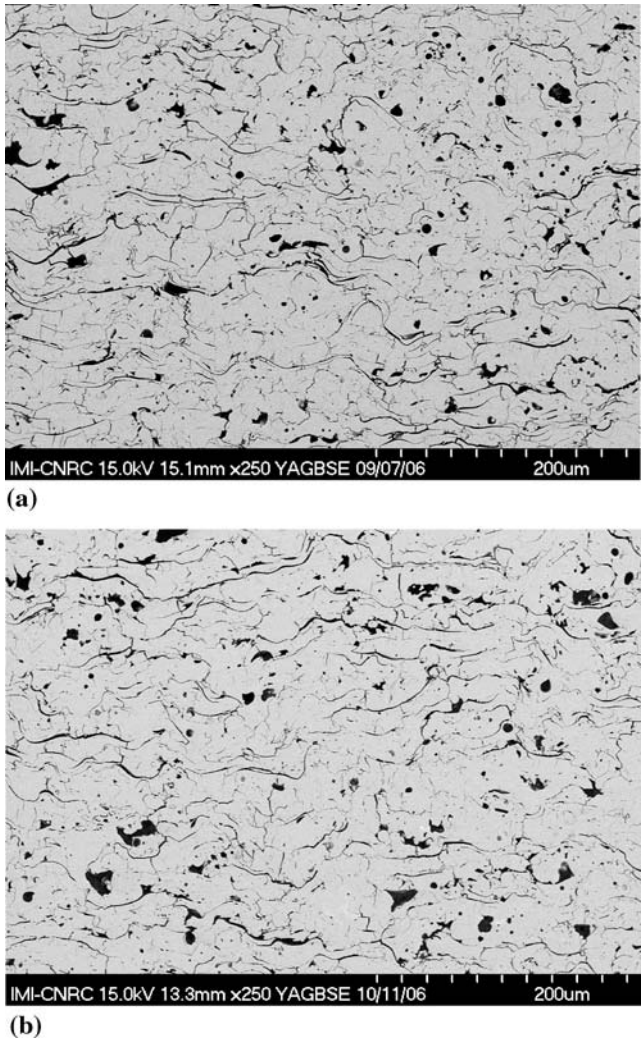

Fig. 10 Microstructure of a coating deposited using spray parameter Set 12 (N_2, see Table 2) in the as-sprayed state (a) and following 20 h at 1400 °C (b)

behaved differently with regard to phase stability (and rate of phase change) at elevated temperatures.

Therefore, a number of possible explanations exist for the observed differences in the properties between the two series of coatings. Further analyses are required to determine if one of the aspects suggested above is causing the differences, if a combination of these factors is involved or if other mechanisms are giving rise to the observed changes in behaviour.

3.4 Microstructure

Micrographs of coatings produced using the two primary plasma gases are shown in Fig. 9 and 10 in both the as-sprayed state and following a 20 h thermal treatment at 1400 °C. The conditions used for depositing these coatings were considered to be typical of those currently employed for these two primary gases. The coatings had similar hardness values; however, the Young's modulus and thermal diffusivity following heat treatment were lower for the coating produced using N_2. The porosity level, as determined by image analysis, was ~5% in both coatings in the heat-treated state. As well, the DE value for the N_2-sprayed coating was more than twice that for the Ar-sprayed coating. Although further testing in simulated operating conditions is required, these results indicate the potential for improving the DE while producing good quality coatings by using N_2. The research also suggests that for users who are currently employing Ar as the primary plasma gas there is merit in exploring the possibility of using nitrogen as an alternate processing route.

4. Conclusions

This research has shown that when producing TBCs with an N_2/H_2 plasma gas mixture, higher in-flight particle temperatures and lower particle velocities are produced as compared with Ar/H_2 plasmas. Coatings having similar values of porosity, hardness, Young's modulus,

and thermal diffusivity can be produced using the two primary gases. Thermal treatments at 1400 °C produced a hardening and stiffening of the coatings and an increase in the thermal conductivity, particularly in the earlier stages of heat treatment. These changes were attributed to enhanced inter-splat contact/bonding. Results also indicated that coatings produced using N_2 might undergo less stiffening and smaller increases in thermal conductivity during the heat treatment. The substantial increase (2×) in DE that can be achieved by using N_2 as the primary plasma gas, together with the possibility of producing coatings having similar (or improved) properties, provides a compelling case (based on powder consumption and production rate) for using nitrogen as the primary plasma gas for TBC deposition.

Acknowledgments

The authors thank J. F. Alarie, S. Bélanger, F. Belval, B. Harvey, M. Lamontagne, M. Lord and M. Thibodeau for technical support in executing this research.

References

1. A. Feuerstein, J. Knapp, T. Taylor, A. Ashary, A. Bolcavage, and N. Hitchman, Thermal Barrier Coating Systems for Gas Turbine Engines by Thermal Spray and EBPVD—A Technical and Economic Comparison, pdf format, Paper s16_3-11673, *Building on 100 Years of Success: Proceedings of the 2006 International Thermal Spray Conference*, B.R. Marple, M.M. Hyland, Y.C. Lau, R.S. Lima, and J. Voyer, Eds., May 15-18, 2006 (Seattle, WA, USA), ASM International, Materials Park, OH, USA, 2006
2. J.F. Bisson, C. Moreau, M. Dorfman, C. Dambra, and J. Mallon, Influence of Hydrogen on the Microstructure of Plasma-Sprayed Yttria-Stabilized Zirconia Coatings, *J. Thermal Spray Technol.*, 2005, **14**, p 85-90
3. A.S. Houlbert, P. Cielo, C. Moreau, and M. Lamontagne, Measurement of Thermal Diffusivity and Anisotropy of Plasma-Sprayed Coatings, *Int. J. Thermophys.*, 1994, **15**, p 525-546
4. C. Bescond, S.E. Kruger, D. Lévesque, R.S. Lima, and B.R. Marple, In-Situ Simultaneous Measurement of Thickness, Elastic Moduli and Density of Thermal Sprayed WC-Co Coatings by Laser-Ultrasonics, *J. Thermal Spray Technol.*, 2007, **16**(2), p 238-244
5. M.I. Boulos, P. Fauchais, and E. Pfender, Thermal Plasmas: Fundamentals and Applications, Vol 1. Plenum Press, NY, USA, 1994
6. H.G. Scott, Phase Relationships in the Zirconia-Yttria System, *J. Mater. Sci.*, 1975, **10**, p 1527-1535
7. R.A. Miller, J.L. Smialek, and R.G. Garlick, Phase Stability in Plasma Sprayed Partially Stabilized Zirconia-Yttria. A.H. Heuer and L.W. Hobbs Eds., *Advances in Ceramics, Vol 3—Science and Technology of Zirconia*, Columbus, OH, USA: American Ceramic Society, 1981, p 241-253
8. D.R. Clarke and C.G. Levi, Materials Design for the Next Generation Thermal Barrier Coatings, *Annu. Rev. Mater. Res.*, 2003, **33**, p 383-417